Marcon, L., Soriano-Amat, M., Veronese, R., García-Ruiz, A., Calabrese, M., Costa, L., Fernández-Ruiz, M.R., Martins, H.F., Palmieri, L. & González-Herráez, M. 2020, "Analysis of disturbance-induced 'virtual' perturbations in chirped pulse ϕ-OTDR", IEEE Photonics Technology Letters, vol. 32, no. 3, pp. 158-161

Available at http://dx.doi.org/10.1109/LPT.2019.2963219

Analysis of disturbance-induced "virtual" perturbations in chirped pulse ϕ-OTDR

Leonardo Marcon, Miguel Soriano-Amat, Riccardo Veronese, Andres Garcia-Ruiz, Marco Calabrese, Luis Costa, Maria R. Fernandez-Ruiz Hugo F. Martins, Luca Palmieri, and Miguel Gonzalez-Herraez

***Abstract*—When a disturbance acts on a fiber it induces a change in the local refractive index that influences the fiber backscattering trace. If a chirped pulse ϕ-OTDR setup is used to interrogate the fiber, this refractive index change appears as a local shift of the received trace, linear to the acting perturbation. However, the refractive index change influences the round trip time of all the backscattering components generated by further fiber sections as well. Due to the high sensitivity of chirped pulse ϕ-OTDR, the change in the round trip time of the backscattering components, which is usually negligible, may appear as a virtual perturbation in certain conditions.**

In this letter we derive a mathematical model for the virtual perturbation induced by a disturbance acting on the fiber, when the measurement is performed by a chirped pulse ϕ-OTDR. We experimentally validate the model by inducing a temperature change on a known span of fiber while monitoring its effects in a further fiber section kept at rest. The experimental results are then analyzed and compared with the theoretical ones.

***Index Terms*—Distributed Acoustic Sensing, Phase-sensitive Optical Time Domain Reflectometry, Rayleigh scattering**

I. Introduction

THE characteristics of the optical fiber, namely its robustness, insensitivity to electromagnetic disturbances and vast multiplexing capacity have constantly spurred interest in the development of high-performance distributed fiber sensors. Distributed measurements are possible thanks to the intrinsic fiber backscattering phenomena [1] that allow to collect information about perturbations, like temperature changes or vibrations [2], acting along the whole fiber.

A common setup, based on Rayleigh backscattering, used to realize distributed acoustic sensing (DAS) is called phase-sensitive optical time domain reflectometer (ϕ-OTDR) [3]. It usually exploits a sequence of flat-phase coherent light pulses to investigate tens of kilometers of fiber with spatial resolutions of meters and acoustic bandwidths of few kilohertz. Standard ϕ-OTDRs exploiting flat-phase input pulse and direct-detection cannot perform a linear analysis of the perturbations acting on the fiber due to the amplitude based measurement procedure they implement, and they do not provide reliable information for all those positions where, due to coherent fading [4], the magnitude of the backscattered trace generated is low [5]. To mitigate these issues specific techniques were developed [5], [6], but a significant improvement of the ϕ-OTDR performance came with the introduction of the technique called chirped pulse ϕ-OTDR (CP ϕ-OTDR) [7]. In CP ϕ-OTDR the instantaneous frequency of the light pulses is linearly chirped, transforming the measurement procedure into a time-delay estimation which guarantees perfect linearity and temperature/strain sensitivities in the order of millikelvin/nanostrain. Such sensitivities increase the impact of distortions so far considered negligible, like the cumulative round-trip time changes induced by perturbations acting on the fiber on all the backscattering components generated from further fiber sections. While the measurement error induced by such distortion is negligible in the majority of cases, even where long perimeters are monitored [8][9], if a section of the fiber undergoes an intense environmental perturbation, like a distributed temperature change caused over tens of kilometers of fiber by the daylight cycle, it may become significant. While in other setup the cumulative round-trip time change does not influence significantly the measure, in the measurement performed with a CP ϕ-OTDR it appears as a distributed, homogeneous, virtual perturbation that may potentially be corrected using a suitable model.

The aim of this letter is to derive and experimentally validate a model for the virtual perturbation induced by the cumulative round-trip time delay change. We start by mathematically describing the changes in the refractive index induced by a disturbance acting on the fiber and then we consider how they propagate in the theoretical measurement procedure of the CP ϕ-OTDR to derive the model of the corresponding virtual perturbation. We then realize an experiment where the CP ϕ-OTDR monitors two sections of a standard fiber, the first experiencing a temperature change and the second kept at rest. The theoretical results obtained from feeding the model with the temperature change applied on the first section of the fiber are validated by comparing them with the virtual perturbation measured on the second section of the fiber. The proposed model can be exploited by an algorithm that for each measured disturbance computes and correct the corresponding virtual perturbation, improving the quality of the CP ϕ-OTDR.

II. Theoretical Model

As the input pulse $P(t,z)$ of a CP ϕ-OTDR, with central frequency ν_0, total chirp applied δ_ν and width τ_p propagates along the fiber, a small portion of its power $B(t)$ gets back-reflected due to Rayleigh backscattering. The round-trip time of the light $t_{RT}(z)$ is accurately measured:

$$t_{RT}(z) = 2\int_0^z \frac{n(\zeta)}{c} d\zeta, \tag{1}$$

L. M., R. V., M. C. and L. P. are with the Department of Information Engineering (DEI), University of Padova, Italy. (leonardo.marcon.1@phd.unipd.it)

M. S.-A., A. G.-R., L. C., H. F. M. and M. G.-H. are with the Departamento de Electronica, Universidad de Alcala', Spain

This article has been accepted for publication in a future issue of this journal, but has not been fully edited. Content may change prior to final publication. Citation information: DOI 10.1109/LPT.2019.2963219, IEEE Photonics Technology Letters

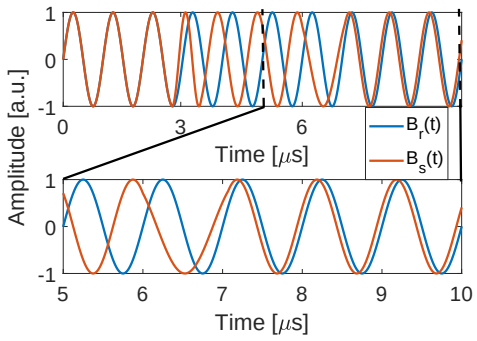

(a)

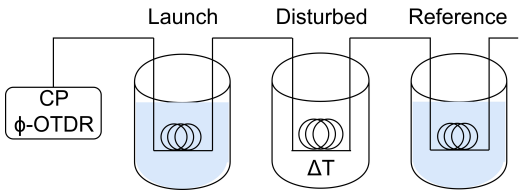

(b)

Fig. 1. (a) Consequences of a localized disturbance on a simplified $B(t)$. On the bottom is shown a detail of the traces after the perturbation; (b) Schematic representation of the setup.

where $n(z)$ is the refractive index of the fiber and used to map each contribution of $B(t)$ to the positions of the fiber that generates it. While the fiber is kept at rest, consecutive interrogations with identical input pulses always generate the same backscattering trace $B(t)$. Differently, when a perturbation $\xi(t)$ acts on an arbitrary section of the fiber $I = [z_i, z_j]$, due to thermo-optic and/or elasto-optic effects the local refractive index $n(I)$ changes by $\Delta n(t)$. Considering then a reference backscattering trace $B_r(t)$ acquired before the perturbation and a disturbed backscattering trace $B_s(t)$ acquired during the perturbation, the difference they will present is a local shift induced by $\Delta n(t)$ on $B_s(t)$ for all $t = t_{RT}(I)$. This difference is represented in the first plot of Fig. 1a where the reference and disturbed traces are perfectly overlapped until $t = 3$ μs when a shift appears. In chirped-pulse ϕ-OTDR the measurement begins by dividing both $B_r(t)$ and $B_s(t)$ into corresponding windows. For each couple of corresponding windows, that represent different positions of the fiber, a cross-correlation operation is performed, and all the resulting central peaks are monitored. Due to the shift introduced by $\Delta n(t)$ in $B_s(t)$, the correlation peaks of the couples of windows corresponding to the fiber section I will shift by Δt:

$$\frac{\Delta n(t)}{n} = -\left(\frac{1}{\nu_0}\right)\left(\frac{\delta\nu}{\tau_p}\right)\Delta t. \tag{2}$$

By measuring the time-delay Δt and inverting eq. (2), it is possible to extract the value of $\Delta n(t)$ which is linearly proportional to the perturbation disturbing the fiber. Due to the sensitivity of the correlation operation, the CP ϕ-OTDR allows to sense temperature and strain changes with resolutions in the order of few millikelvin and nanostrain respectively. From eq. (1) it can be seen that the refractive index change in the section I of the fiber causes a corresponding change $\Delta t_{RT}(t)$ common to all position $z > z_j$. This distortion induces a small shift to all the corresponding components of $B_s(t)$ as visualized in detail in the second plot of Fig. 1a, where after $t > 7\mu$s, even if no perturbation is applied, the two traces are not as perfectly overlapped as they were at the beginning. The time-delay estimation procedure described above will identify this small delay as a "virtual" perturbation, i.e. as a measured perturbation when there is no real applied disturbance in that fiber section. Luckily, this virtual perturbation will generally be negligible in realistic settings, and moreover can be easily corrected as we will show below.

It is convenient to develop the theoretical model describing the virtual perturbation starting from a temperature change, since it allows to reach a more general expression. It will be immediate afterwards to derive the equations of the virtual perturbation when the original perturbation is a strain. When a section of fiber L at room temperature experiences a temperature change $\Delta T(t)$ the length of the fiber changes due to thermal expansion, $\tilde{L}(t) = L + \Delta L(t)$, and the local refractive index changes due to the thermo-optic effect, $\tilde{n}(t) = n + \Delta n(t)$. The linear length variation $\Delta L(t) = \alpha \Delta T(t) L$ can be estimated through the amorphous silica linear thermal expansion coefficient $\alpha \approx 0.55 \times 10^{-6}$ [$^{\circ}C^{-1}$] [10], while the linear refractive index change $\Delta n(t) = \zeta_T \Delta T(t) n$ is proportional to the thermo-optic coefficient of the fiber $\zeta_T = \approx 6.92 \times 10^{-6}$ [11]. The common round-trip time shift $\Delta t_{RT}(t)$ for all positions after $\tilde{L}(t)$ can then be expressed as:

$$\begin{aligned}\Delta t_{RT}(t) &= 2\left[\int_0^{\tilde{L}(t)} \frac{\tilde{n}(t)}{c} dz - \int_0^{L} \frac{n}{c} dz\right] = \\ &= 2\frac{\tilde{n}(t)\tilde{L}(t)}{c} - 2\frac{nL}{c} \approx 2\frac{n\Delta L(t)}{c} + 2\frac{\Delta n(t) L}{c}\end{aligned} \tag{3}$$

where the term proportional to $\Delta n(t)\Delta L(t)$ is neglected since it is many orders of magnitude lower than the others. According to eq. (2), the round trip time delay change $\Delta t_{RT}(t)$ appears to the instrument as caused by a distributed, homogeneous, virtual temperature change $\delta T(t)$ that modifies the refractive index of the fiber for all positions after $z > z_j$:

$$-\left(\frac{1}{\nu_0}\right)\left(\frac{\delta\nu}{\tau_p}\right)\Delta t_{RT}(t) = \frac{\Delta n_{RT}(t)}{n} = \zeta_T \delta T(t). \tag{4}$$

By substituting eq. (3) in (4), and solving for $\delta T(t)$ we get:

$$\begin{aligned}\delta T(t) =& K\frac{1}{\zeta_T}\frac{1}{\nu_0}\frac{\delta\nu}{\tau_p}\left[2\frac{n\Delta L(t)}{c} + 2\frac{\Delta n(t) L}{c}\right] = \\ & K\frac{1}{\zeta_T}\frac{1}{\nu_0}\frac{\delta\nu}{\tau_p}\frac{2nL}{c}\left[\alpha\Delta T(t) + \zeta_T \Delta T(t)\right].\end{aligned} \tag{5}$$

where the first term is related only to the thermal expansion and the second only to the thermo-optic effect. The two terms differ only for the coefficients α and ζ_T, thus the contribution of the thermo-optic effect on $\delta T(t)$ is about one order of magnitude

This article has been accepted for publication in a future issue of this journal, but has not been fully edited. Content may change prior to final publication. Citation information: DOI 10.1109/LPT.2019.2963219, IEEE Photonics Technology Letters

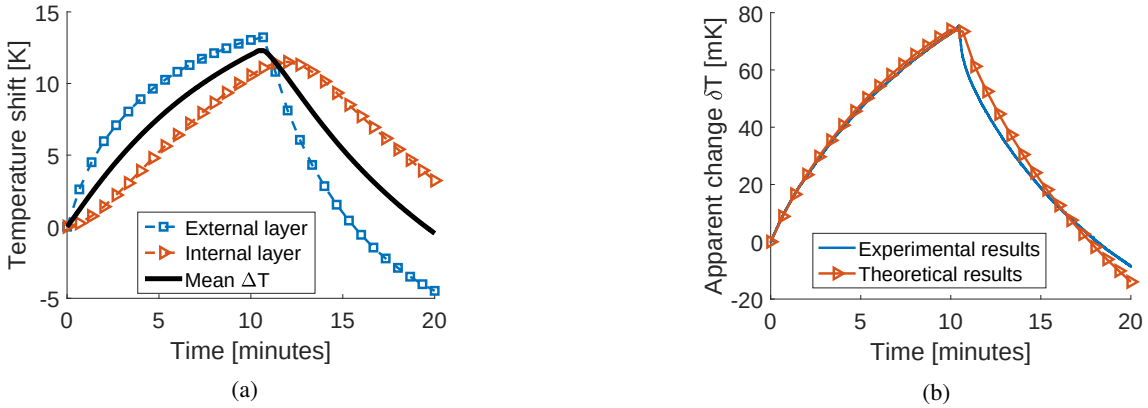

(a) (b)

Fig. 2. (a) Temperature changes in the disturbed fiber measured in different positions (marked lines); Mean temperature change of the disturbed fiber (black solid line). (b) Measured virtual temperature change in the reference fiber (blue line) compared with the expected result (marked red line).

higher than the one induced by thermal expansion. A constant scaling factor K has been added in the model because the actual values of the thermo-optic coefficient ζ_T and of the thermal expansion coefficient α of the fiber used may differ slightly from the values reported in the literature. As can be seen in eq. (5), the magnitude of the virtual perturbation depends linearly on the characteristics of the original perturbation applied, namely L and $\Delta T(t)$, and on the sensitivity of the instrument, defined by the chirp rate $\delta\nu/\tau_p$. By using common operating parameters, i.e. a pulse width $\tau_p = 100$ ns, a total applied chirp of $\delta\nu = 1$ GHz, a central frequency of the laser of $\nu_0 = 193$ THz and a fiber of length $L = 20$ km, a temperature change ΔT of few kelvin degrees can generate a virtual temperature change of tens of millikelvin, which is small but still more than 10 times the accuracy of the instrument.

When strain is the original perturbation considered $\Delta\varepsilon(t)$, the virtual change can be derived from (3) observing that $\Delta L = \Delta\varepsilon(T)L$ and $\Delta n(t) = \gamma\Delta\varepsilon(t)n$ where $\gamma = -0.22$ is the fiber elasto-optic coefficient:

$$\delta\varepsilon(t) = K\frac{1}{\zeta_\varepsilon}\frac{1}{\nu_0}\frac{\delta\nu}{\tau_p}\frac{2nL\Delta\varepsilon(t)\,(1+\gamma)}{c}. \tag{6}$$

$\zeta_\varepsilon = 1 + \gamma = 0.78$ [11] is a composite coefficient, which includes both the elasto-optic effect and the fiber deformation, consistent with the value reported in the literature [11].

III. Experimental Setup

The setup used to validate the model is schematically represented in Fig. 1b, where a standard fiber of total length $L = 18.6$ km, divided into three different sections called respectively launch, disturbed and reference, is connected to a standard CP ϕ-OTDR [7]. The laser source, centered at a wavelength of $\lambda_0 = 1.55$ μm, is modulated at a rate of $F_s = 1000$ Hz to generate chirped pulses with a width of $\tau_p = 100$ ns and a total applied chirp of $\delta\nu = 1$ GHz. Such parameters, which are left untouched during the whole experiment, guarantee good SNR and sensitivity over the whole length of the fiber, while limiting resources and storage capacity consumption. The launch fiber is $L_L = 0.9$ km long and it is kept at rest to acquire an estimate of the laser phase noise, used in post-processing to correct all the measurement taken from the other fiber sections [12]. The temperature change $\Delta T(t)$ is induced on the disturbed fiber, which is $L_S = 16.3$ km long, by submerging it in warm, and successively cold, water. Finally, the reference fiber, which is $L_R = 1.4$ km long, is used to measure the virtual perturbation $\delta T(t)$ induced by the previous temperature change $\Delta T(t)$. As can be seen from Fig. 1b, the launch and reference fibers are immersed into room temperature water, represented by a light blue color, to partially isolate them from external perturbations. The choice of using water to induce the temperature change $\Delta T(t)$ in the disturbed fiber L_S is due to the high thermal capacity of water. A fast thermalization of the disturbed fiber is important since it speeds up the experiment, reducing the impact of instrument-related noise and remaining environmental noise on the measurement. To avoid the effect of floating of the coils during the experiment, a little weight is leaned on their top, thus anchoring them to the bottom of the buckets.

IV. Results

The measurement started by submerging the disturbed fiber L_S in a bucket containing water at a temperature $T_H \approx 15$ K higher than the room temperature. To allow a sufficient thermalization the setup was left resting for 10 minutes, then the fiber was moved from the warm water to the cold, at a temperature $T_C \approx 8$ K lower than the room temperature, for 10 more minutes. The amount of water in the buckets was enough to consider the water temperatures as constants during the thermalization process. The cool-down phase provides a further proof that the virtual perturbation in the reference fiber is indeed induced by the temperature change in the disturbed fiber and not related to random environmental changes. Due to the fiber low thermal conductivity and its coiled geometry, the temperature change experienced by the different layers of the disturbed fiber L_S is not uniform and the CP ϕ-OTDR measures a position-depended perturbation $\Delta T(z,t)$. This is clearly visible in Fig. 2a where the temperature changes measured at an outer (blue line, square marker) and inner (red line, triangular marker) layer, are represented. As can be seen, during both thermal phases the temperature of the layer closer to the water

This article has been accepted for publication in a future issue of this journal, but has not been fully edited. Content may change prior to final publication. Citation information: DOI 10.1109/LPT.2019.2963219, IEEE Photonics Technology Letters

shows an immediate exponential-like response, which agrees with the Newtonian laws of heating and cooling, while the change in the inner one is delayed and shows an almost linear change corresponding to the same exponential behavior but with a much larger time constant. Since both the thermo-optic effect and thermal expansions are linear with respect to the temperature, it is convenient to average the position-dependent perturbations $\Delta T(z,t)$ into an equivalent uniform temperature change $\Delta T(t)$, reported in Fig. 2a as a black solid line.

The apparent perturbations $\delta T(z,t)$ induced by the temperature change in the disturbed fiber are measured along the whole reference fiber. Due to instrument-related noise and remaining environmental disturbed, the terms $\delta T(z,t)$ along the reference fiber represent position-dependent replicas of the same virtual perturbation with an added, arbitrary, temporal evolution, which can be averaged to obtain the desired $\delta T(t)$. The results are shown in Fig. 2b (N=100 replicas were averaged) where the experimental virtual perturbation (blue solid line) is compared with the theoretical one (red marked line). The theoretical curve was computed using the model of eq. (5) with $K = 0.78$, $\Delta L = L_S$ and the equivalent uniform temperature change measured in the disturbed fiber $\Delta T(t)$ as parameters. As can be seen, the curves show a great agreement during the whole experiment, even if a slight mismatch is visible during the cool down. Furthermore, the magnitude of the virtual perturbations matches the expected order of magnitude computed in the theoretical model section. The mismatch between the two curves can be explained by several reasons: position-dependent ambient noise, strain induced in the fiber during the bucket exchange phase, imperfect reference updating [7], etc. These effects can be smoothed down by the averaging operation of the terms $\delta T(z,t)$ along the position axis, but cannot be completely removed. The increasing difference in time between the traces is better visualized by computing the standard deviation of the $\delta T(z,t)$ terms along the position axis for each time instant. The result is shown in Fig. 3, where the instant standard variation is added to the averaged measurement. As can be noticed, the standard deviation is monotonically growing in time, with the cumulation of all the sources of drift.

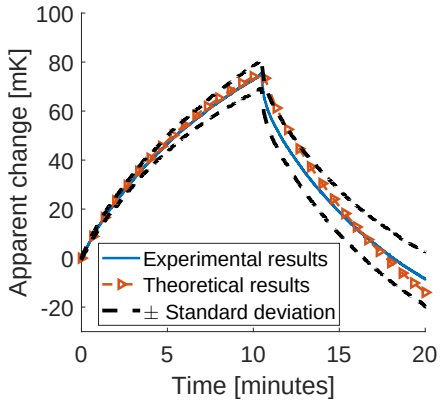

Fig. 3. Experimental data with standard deviation bounds.

V. Conclusion

In this letter we have proposed a mathematical model of the disturbance-induced virtual perturbation measured by a CP ϕ-OTDR. The parameters of the model, which depends on the original disturbance and on the measurement procedure of the instrument, have been highlighted and discussed. We have then performed an experiment where the temperature of a known section of fiber was changed, and the consequent virtual perturbation has been monitored. The theoretical results were compared with the experimental ones showing a convincing agreement. The proposed model can be used to estimate and progressively correct the errors introduced by perturbations acting on the fiber, thus improving the quality of the measurement performed with CP ϕ-OTDR, especially when weak perturbations are being monitored. Nevertheless, it should be noted that the effect of these "induced virtual perturbations" should be negligible in the vast majority of practical cases, since the values of disturbance required to observe these "virtual" perturbations are quite high in comparison with the type of stimuli that can be induced in regular field installations.

Acknowledgment

This work was supported by project FINESSE MSCA-ITN-ETN-722509; the DOMINO Water JPI project under the WaterWorks2014 cofounded call by EC Horizon 2020, the Spanish MINECO and Italian MIUR; Comunidad de Madrid and FEDER Program (P2018/NMT-4326); project TEC2015-71127-C2-2-R and RTI2018-097957-B-C31; HFM acknowledges financial support from the Spanish Ministery (MICINN) under contract no. IJCI-2017-33856; LM acknowledge Fondazione Ing. Aldo Gini for partial support; AGR acknowledge the University of Alcala' for partial support (FPI).

References

[1] X. Bao and L. Chen, "Recent Progress in Distributed Fiber Optic Sensors, Sensors," vol. 12, no. 7, pp. 8601-8639, Jun 2012.
[2] J. A. Bucaro and T. R. Hickman, "Measurement of sensitivity of optical fibers for acoustic detection," Appl. Opt., vol. 18, no. 6, pp. 938-940, Mar 1979.
[3] J. C. Juarez *et al.*, "Distributed fiber-optic intrusion sensor system," J. Light. Technol., vol. 23, no. 6, pp. 2081-2087, Jun 2005.
[4] P. Healey, "Fading in heterodyne OTDR," Electron. Lett., vol. 20, no.1, pp. 30-32, Jan 1984.
[5] H. Gabai and A. Eyal, "On the sensitivity of distributed acoustic sensing," Opt. Lett., vol. 41, no. 24, pp. 5648-5651, Dec 2016.
[6] H. F. Martins *et al.*, "Coherent Noise Reduction in High Visibility Phase-Sensitive Optical Time Domain Reflectometer for Distributed Sensing of Ultrasonic Waves," J. Light. Technol., vol 31, no. 23, 3631–3637, Dec 2013.
[7] J. Pastor-Graells *et al.*, "Single-shot distributed temperature and strain tracking using direct detection phase-sensitive OTDR with chirped pulses," Opt. Express, vol. 24, no. 12, 13121, Jun 2016.
[8] J. C. Juarez and H. F. Taylor, "Field test of a distributed fiber-optic intrusion sensor system for long perimeters," Appl. Opt., vol. 46, no. 11, pp. 1968-1971, May 2007.
[9] F. Peng *et al.*, "Ultra-long high-sensitivity ϕ-OTDR for high spatial resolution intrusion detection of pipelines," Opt. Express, vol. 22, no. 11, pp. 13804-13810, Jun 2014.
[10] G. K. White, "Thermal expansion of reference materials: copper, silica and silicon," J. Phys. D, vol. 6, no. 17, pp. 2070-2078, Nov 1973.
[11] Y. Koyamada *et al.*, "Fiber-Optic Distributed Strain and Temperature Sensing With Very High Measurand Resolution Over Long Range Using C-OTDR," J. Light. Technol., vol. 27, no. 9, pp. 1142-1146, May 2009.
[12] M. R. Fernández-Ruiz *et al.*, "Laser Phase-Noise Cancellation in Chirped-Pulse Distributed Acoustic Sensors," J. Light. Technol., vol. 36, no. 4, pp. 979-985, Feb 2018.